Asian Pub. Corp.

www.asianpubs.org

ARTICLE

# Synthesis, Structural, Spectral, Natural Bond Orbital, Thermodynamic Properties and First Order Hyperpolarizability Analysis of N-(4-Chlorobenzylidene)-4-methoxyaniline

Golda Louis and A.S. Haja Hameed✉

**Asian Journal of Organic & Medicinal Chemistry**

Volume: 2 Year: 2017
Issue: 4 Month: October–December
pp: 169–181
DOI: https://doi.org/10.14233/ajomc.2017.AJOMC-P88

Received: 8 June 2017
Accepted: 28 November 2017
Published: 29 December 2017

## ABSTRACT

A potential non-linear optical (NLO) material N-(4-chlorobenzylidene)-4-methoxyaniline (CBMA) was synthesized by the condensation reaction between *p*-chlorobenzaldehyde and *p*-methoxyaniline. The CBMA crystal was grown by slow evaporation method for the period of 30 days. The optimized geometry and structural features of the title compound CBMA were thoroughly described with the FT-Raman and FT-IR spectra calculated by the HF/DFT/B3LYP methods using 6-311G(d,p) as basis set. The theoretical, experimental FT-IR and FT-Raman spectra were compared. A natural bond orbital (NBO) study was carried out to analyze the effects of intramolecular charge transfer. The effects of frontier orbitals, HOMO and LUMO, transition of electron density transfer were discussed. The first order hyper polarizability ($\beta_0$) and related properties ($\beta$, $\alpha_0$ and $\mu$) of CBMA were calculated. Molecular electrostatic potential was studied using theoretical calculations. The thermodynamic properties (heat capacity, entropy and enthalpy) at different temperatures were also calculated.

## KEYWORDS

N-(4-Chlorobenzylidene)-4-methoxyaniline, HF, DFT/B3LYP, Molecular electrostatic potential, Hyperpolarizability.

## INTRODUCTION

Schiff bases have been used as ligands in the field of coordination chemistry [1] and have antimicrobial [2] and anticancer applications [3]. Schiff base compounds make an interest by the formation of intramolecular hydrogen bonds by electron coupling between acid-base centers [4] and corrosion inhibition mechanism [5]. The electron donor and the acceptor groups connected through a π conjugated chain constitute a potential non-linear optical (NLO) or an electro-optical material. The synthesis of organic molecules exhibiting NLO properties has been encouraged by their optical and electronic applications [6,7]. Organic molecules with significant non-linear optical activity generally consist of π-electron conjugated moiety which is substituted by an electron donor group on one end of the conjugated structure and an acceptor group on the other end. It makes a push-pull conjugated structure. Both ends of the π-bond system functionalizing with appropriate electron donor and acceptor groups lead to an increase in optical non-

***Author affiliations:***

PG and Research Department of Physics, Jamal Mohamed College, Tiruchirappalli-620 020, India

✉To whom correspondence to be addressed:

Fax: +91-431-233145
Tel: +91 431 2331135; +91 431 2332235
E-mail: hajahameed2001@gmail.com

Available online at: http://ajomc.asianpubs.org

linearity [8-11]. For effective second harmonic generation (SHG), one requires a highly polarizable molecular system with asymmetric charge distribution in the molecule. Benzylideneaniline (BA) derivatives are successful examples for preparing high non-linear optically active crystals [12-15]. Among many NLO crystals, N-(4-chlorobenzylidene)-4-methoxyaniline (CBMA) is one of benzylideneaniline derivative NLO crystals, which belongs to the non-centrosymmetric orthorhombic space group $Pna2_1$. The cell dimensions [16] are a = 6.11 Å, b =7.34 Å, c =27.47 Å and V = 1230.9 $Å^3$.

In this paper, we have performed geometry optimization calculations for the CBMA molecule by using HF and DFT/B3LYP methods with 6-311G(d,p) basis set. We have accomplished an experimental/theoretical analysis of the vibrational spectra. Also, the paper explores the molecular dynamics and the structural parameters that concern the chemical behaviour.

## EXPERIMENTAL

**Synthesis:** N-(4-Chlorobenzylidene)-4-methoxyaniline (CBMA) was synthesized by the condensation reaction between *p*-chlorobenzaldehyde and *p*-methoxyaniline in equimolar ratio [16]. The reaction mixture was refluxed for 8 h and the solution was filtered using a Whatmann filter paper and the resulting product N-(4-chlorobenzylidene)-4-methoxyaniline was obtained. The schematic diagram of synthesizing CBMA material is shown in Fig. 1. The purity of the synthesized salt was improved by successive recrystallization processes in ethanol and acetone (1:1) at room temperature. A transparent single crystal grown for the period of 30 days by slow evaporation at room temperature is shown in Fig. 2.

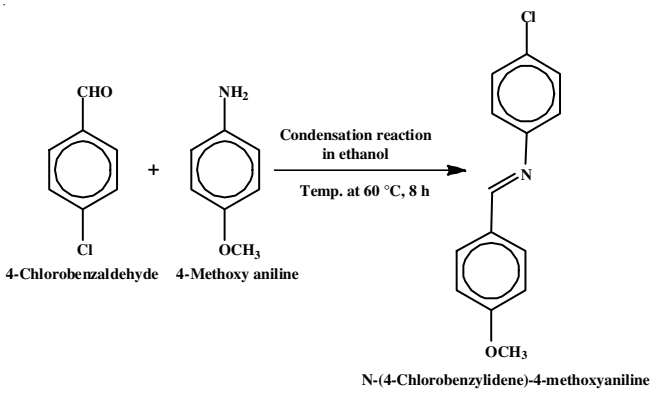


Fig. 1. Schematic of synthesizing CBMA material

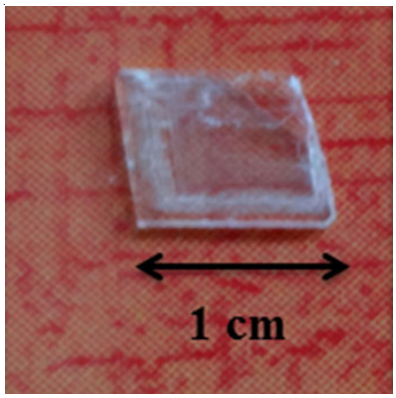


Fig. 2. Grown crystal of CBMA

**FT-IR and FT-Raman spectral measurements:** The FT-IR spectrum of CBMA sample was recorded in the range of 4000-400 $cm^{-1}$ by Perkin Elmer, RXI model FT-IR spectrometer using KBr pellet technique. FT-Raman spectrum of CBMA sample was recorded using 1064 nm line of Nd:YAG laser as the excitation wavelength in the region 3500-50 $cm^{-1}$ by BRUKER RFS 27: FT-Raman spectrometer.

**Computational details:** The optimization of the molecular structure and its vibrational harmonic frequencies of CBMA were calculated using HF/DFT method [17] with the Becke's three-parameter hybrid functional (B3) [18] for the exchange part and the Lee-Yang-Parr (LYP) correlation function [19] using the Gaussian 09 program [20]. At first, the molecule N-(4-chlorobenzylidene)-4-methoxyaniline was optimized. Then the optimized structural parameters were calculated. The vibrational wavenumber assignments were done. The calculated IR spectrum of CBMA was plotted using Origin Pro 8.1 and compared with the experimental FT-IR spectrum.

The natural bonding orbital (NBO) calculations [21] were performed using Gaussian 09 [20] to understand different second order interactions between the vacant orbitals of one subsystem and filled orbitals of another subsystem. UV-visible spectra, electronic transitions, excitation energies and oscillator strengths were computed with the time-dependent DFT method. The HOMO and LUMO energies were determined. To investigate the reactive sites of the title compound, the MEP was evaluated using the DFT/B3LYP method. The contribution of the group to a molecular orbital was analyzed using Mulliken population analysis. The first order hyperpolarizability ($\beta_0$) and related properties ($\beta$, $\alpha_0$ and $\mu$) were calculated using 6-311G(d,p) basis set based on the finite-field approach [22]. The thermodynamic functions such as heat capacity, entropy and enthalpy were analyzed for different temperatures.

**Prediction of Raman intensities:** The measured Raman spectrum is given by the equation [23,24]. The Raman activities (Si) calculated by Gaussian 09 program [20] have been converted to corresponding Raman intensities ($I^R$). The theoretical Raman intensity ($I^R$) that simulates is given by

$$I_i^R = C(\nu_0 - \nu_i)^4 \nu_i^{-1} B_i^{-1} S_i \quad (1)$$

where $B_i$ is a temperature factor for the intensity contribution of excited vibrational states and the excitation frequency $\nu_0$ = 9398.5 $cm^{-1}$ corresponds to the wavelength of 1064 nm of Nd:YAG laser, $\nu_i$ is the frequency of normal mode ($cm^{-1}$), while $S_i$ is the Raman scattering activity of the normal mode Qi. $I_i^R$ is given in arbitrary units (C is a constant equal $10^{-12}$). Theoretical Raman intensities have been computed assuming $B_i$ equal to 1. The theoretical Raman spectra have been calculated using HF and DFT/B3LYP/6-311G(d,p).

## RESULTS AND DISCUSSION

**Structural analysis:** The optimized molecular structure of N-(4-chlorobenzylidene)-4-methoxyaniline (CBMA) is shown in Fig. 3. The geometrical parameters (bond lengths, bond angles and dihedral angles) obtained by the HF and DFT-B3LYP/6-311G(d,p) basis set calculations are represented in Table-1. From Table-1, most of the bond lengths are slightly longer than the experimental values and the bond angles are

TABLE-1
CALCULATED OPTIMIZED PARAMETER VALUES OF CBMA [BOND LENGTHS (Å) AND ANGLES (°)

| Bond length | DFT B3LYP | HF | EXP. [Ref. 16] | Bond angle | B3LYP | HF | EXP. [Ref. 16] | Dihedral angle | B3LYP | HF |
|---|---|---|---|---|---|---|---|---|---|---|
| C1-C2 | 1.395 | 1.385 | 1.378 | C2-C1-C6 | 119.99 | 118.86 | 119.42 | C6-C1-C2-C3 | 0.032 | 0.0115 |
| C1-C6 | 1.394 | 1.378 | 1.371 | C2-C1-H7 | 119.99 | 120.84 | 120.30 | C6-C1-C2-H8 | 179.95 | 179.94 |
| C1-H7 | 1.099 | 1.073 | 0.930 | C6-C1-H7 | 120.00 | 120.28 | 120.30 | H7-C1-C2-C3 | -179.97 | -179.9 |
| C2-C3 | 1.394 | 1.386 | 1.381 | C1-C2-C3 | 120.00 | 120.97 | 121.10 | H7-C1-C2-H8 | -0.05 | -0.035 |
| C2-H8 | 1.099 | 1.076 | 0.930 | C1-C2-H8 | 119.98 | 119.08 | 119.50 | C2-C1-C6-C5 | 0.014 | 0.005 |
| C3-C4 | 1.395 | 1.393 | 1.386 | C3-C2-H8 | 120.01 | 119.93 | 119.50 | C2-C1-C6-Cl11 | 179.98 | 179.96 |
| C3-C12 | 1.540 | 1.477 | 1.463 | C2-C3-C4 | 119.99 | 119.06 | 118.70 | H7-C1-C6-C5 | -179.97 | 179.98 |
| C4-C5 | 1.394 | 1.378 | 1.373 | C2-C3-C12 | 120.01 | 119.51 | 119.87 | H7-C1-C6-Cl11 | -0.005 | -0.051 |
| C4-H9 | 1.099 | 1.073 | 0.93 | C4-C3-C12 | 119.99 | 121.42 | 121.40 | C1-C2-C3-C4 | -0.056 | -0.045 |
| C5-C6 | 1.395 | 1.386 | 1.388 | C3-C4-C5 | 119.99 | 120.53 | 120.70 | C1-C2-C3-C12 | 179.96 | 179.89 |
| C5-H10 | 1.099 | 1.073 | 0.93 | C3-C4-H9 | 119.98 | 119.06 | 119.60 | H8-C2-C3-C4 | -179.97 | -179.9 |
| C6-Cl11 | 1.760 | 1.743 | 1.732 | C5-C4-H9 | 120.02 | 120.39 | 119.60 | H8-C2-C3-C12 | -0.141 | -0.032 |
| C12-H13 | 1.098 | 1.086 | 0.93 | C4-C5-C6 | 120.00 | 119.31 | 119.50 | C2-C3-C4-C5 | 0.034 | 0.064 |
| C12-N14 | 1.325 | 1.251 | 1.255 | C4-C5-H10 | 120.01 | 120.75 | 120.30 | C2-C3-C4-H9 | -179.99 | -179.9 |
| N14-C15 | 1.470 | 1.409 | 1.415 | C6-C5-H10 | 119.98 | 119.94 | 120.30 | C12-C3-C4-C5 | -179.98 | -179.8 |
| C15-C16 | 1.395 | 1.390 | 1.386 | C1-C6-C5 | 120.00 | 121.25 | 120.50 | C12-C3-C4-C9 | 0.1876 | 0.1207 |
| C15-C17 | 1.394 | 1.388 | 1.402 | C1-C6-Cl11 | 120.00 | 119.45 | 119.55 | C2-C3-C12-H13 | 0.474 | 1.098 |
| C16-C18 | 1.394 | 1.380 | 1.387 | C5-C6-Cl11 | 119.99 | 119.28 | 119.55 | C2-C3-C12-N14 | -178.64 | -178.1 |
| C16-H19 | 1.099 | 1.074 | 0.930 | C3-C12-H13 | 114.56 | 115.45 | 118.60 | C4-C3-C12-H13 | -179.98 | -178.9 |
| C17-C20 | 1.395 | 1.385 | 1.375 | C3-C12-N14 | 122.71 | 122.56 | 122.78 | C4-C3-C12-N14 | 1.22 | 1.83 |
| C17-H21 | 1.099 | 1.075 | 0.930 | H13-C12-N14 | 122.71 | 121.98 | 118.60 | C3-C4-C5-C6 | -0.121 | -0.047 |
| C18-C22 | 1.395 | 1.386 | 1.377 | C12-N14-C15 | 121.05 | 120.24 | 121.00 | C3-C4-C5-H10 | 179.95 | -179.9 |
| C18-H23 | 1.099 | 1.075 | 0.930 | N14-C15-C16 | 119.99 | 117.79 | 116.83 | H9-C4-C5-C6 | 179.97 | 179.95 |
| C20-C22 | 1.394 | 1.381 | 1.386 | N14-C15-C17 | 124.23 | 123.34 | 125.31 | H9-C4-C5-H10 | 0.0463 | 0.004 |
| C20-H24 | 1.099 | 1.075 | 0.930 | C16-C15-C17 | 118.15 | 118.83 | 117.86 | C4-C5-C6-C1 | 0.0293 | 0.0126 |
| C22-029 | 1.54 | 1.361 | 1.366 | C15-C16-C18 | 121.06 | 120.67 | 122.00 | C4-C5-C6-Cl11 | -179.95 | -179.9 |
| C25-H26 | 1.117 | 1.081 | 0.960 | C15-C16-H19 | 118.26 | 118.73 | 119.00 | H10-C5-C6-C1 | 179.97 | 179.96 |
| C25-H27 | 1.117 | 1.086 | 0.960 | C18-C16-H19 | 121.17 | 120.58 | 119.00 | H10-C5-C6-Cl11 | -0.0273 | -0.003 |
| C25-H28 | 1.117 | 1.086 | 0.960 | C15-C17-C20 | 120.00 | 120.50 | 120.27 | C3-C12-N14-C15 | -177.33 | -178.6 |
| C25-O29 | 1.500 | 1.405 | 1.414 | C15-C17-H21 | 118.91 | 120.04 | 119.90 | H13-C12-N14-C15 | 3.626 | 2.216 |
| | | | | C20-C17-H21 | 119.90 | 119.43 | 119.90 | C12-N14-C15-C16 | -148.45 | -139.3 |
| | | | | C16-C18-C22 | 120.28 | 120.08 | 119.11 | C12-N14-C15-C17 | 34.19 | 42.817 |
| | | | | C16-C18-H23 | 120.01 | 120.62 | 120.40 | N14-C15-C16-C18 | 179.86 | 179.96 |
| | | | | C22-C18-H23 | 119.99 | 119.28 | 120.40 | N14-C15-C16-H19 | 0.714 | 0.826 |
| | | | | C17-C20-C22 | 119.88 | 120.18 | 120.82 | C17-C15-C16-C18 | -2.61 | -2.074 |
| | | | | C17-C20-H24 | 119.13 | 120.55 | 119.60 | C17-C15-C16-H19 | 178.23 | 178.79 |
| | | | | C22-C20-H24 | 120.01 | 119.25 | 119.60 | N14-C15-C17-C20 | 178.93 | 179.19 |
| | | | | C18-C22-C20 | 119.39 | 119.68 | 119.91 | C14-C15-C17-H21 | 1.36 | 0.841 |
| | | | | C18-C22-O29 | 124.77 | 120.26 | 125.07 | C16-C15-C17-C20 | 1.59 | 1.349 |
| | | | | C20-C22-O29 | 120.02 | 120.04 | 115.02 | C16-C15-C17-C21 | -175.96 | -177 |
| | | | | H26-C25-H27 | 108.20 | 109.35 | 109.50 | C15-C16-C18-C22 | 1.746 | 1.47 |
| | | | | H26-C25-H28 | 108.19 | 109.31 | 109.50 | C15-C16-C18-H23 | -179.04 | -178.1 |
| | | | | H26-C25-O29 | 105.84 | 106.89 | 109.50 | H19-C16-C18-C22 | -179.97 | -179.4 |
| | | | | H27-C25-H28 | 109.36 | 108.98 | 109.50 | H19-C16-C18-H23 | 0.041 | 0.912 |
| | | | | H27-C25-O29 | 111.46 | 111.06 | 109.50 | C15-C17-C20-C22 | -0.037 | -0.025 |
| | | | | H28-C25-O29 | 111.53 | 111.18 | 109.50 | C15-C17-C20-H24 | 179.97 | 179.72 |
| | | | | C22-O29-C25 | 118.50 | 115.72 | 118.19 | H21-C17-C20-C22 | 177.87 | 178.33 |
| | | | | | | | | H21-C17-C20-H24 | -1.277 | -1.911 |
| | | | | | | | | C16-C18-C22-C20 | 0.034 | -0.114 |
| | | | | | | | | C16-C18-C22-O29 | -179.99 | -179.1 |
| | | | | | | | | H23-C18-C22-C20 | -179.98 | 179.56 |
| | | | | | | | | H23-C18-C22-O29 | 0.022 | 0.562 |
| | | | | | | | | C17-C20-C22-C18 | -1.21 | -0.603 |
| | | | | | | | | C17-C20-C22-O29 | 179.82 | 178.4 |
| | | | | | | | | H24-C20-C22-C18 | 177.93 | 179.64 |
| | | | | | | | | H24-C20-C22-O29 | -1.03 | -1.35 |
| | | | | | | | | C18-C22-O29-C25 | -90.07 | -87.19 |
| | | | | | | | | C20-C22-O29-C25 | 89.89 | 93.79 |
| | | | | | | | | H26-C25-O29-C22 | 179.99 | 179.91 |
| | | | | | | | | H27-C25-O29-C22 | -59.99 | -60.86 |
| | | | | | | | | H28-C25-O29-C22 | 59.99 | 60.68 |

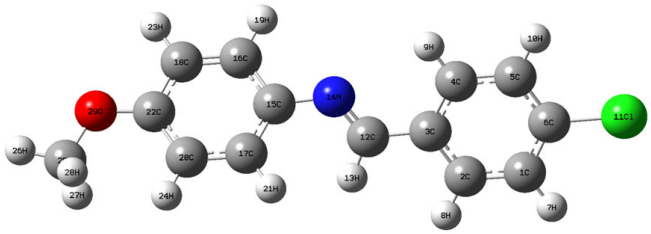

Fig. 3. Theoretical optimized geometric structure with atoms numbering of CBMA

slightly varied from the experimental ones because the states of molecules are different during experimental and theoretical processes. The calculated geometrical parameters showed a good approximation and they can be used to calculate thermodynamic properties and vibrational frequencies, *etc.*

In the benzene ring, C-C bond length is about 1.396 Å [25]. For CBMA, the C-C bond length of the benzene ring varies from 1.394-1.395 Å by B3LYP method, 1.378-1.393 Å by HF method and 1.371-1.402 Å by experimental readings. The C-C bond length of the benzene ring is not similar due to the substitution of methoxy group, chlorine and nitrogen. The aromatic C-H bond lengths such as C1-H7 = 1.099/1.073 Å, C2-H8 = 1.099/1.076 Å, C4-H9 = 1.099/1.073 Å, C5-H10 = 1.099/1.073 Å, C17-H21 = 1.099/1.075 Å, C20-H24 = 1.099/1.075 Å, C16-H19 = 1.099/1.074 Å and C18-H23 = 1.099/1.075 Å are calculated by B3LYP and HF and methods respectively, which is in good agreement with the literature value (0.930 Å) [16]. There are small increments in the C-H bond lengths of the methoxy group (C25-H26 = 1.117/1.081/0.96 Å, C25-H27 = 1.117/1.086/0.96 Å and C25-H28 = 1.117/1.086/0.96 Å calculated by B3LYP, HF and experimental methods, respectively).

The bond length of N14-C12 is 1.325/1.251/1.255 Å calculated by B3LYP, HF and experimental methods respectively, which is shorter than the bond length of N14-C15 (1.47/1.409/1.415 Å by B3LYP, HF and experimental methods); this is due to the double bond between N14 and C12. The C22-O29, C25-O29 bond lengths are 1.54/1.361/1.366 Å and 1.5/1.405/1.414 Å calculated by B3LYP, HF and experimental methods respectively. The bond length of C6-Cl11 is 1.760/1.743/1.732 Å calculated by B3LYP, HF and experimental methods, respectively and this is the longest bond while comparing with all other bonds in the title molecule. Due to the electron donating nature of methoxy group, the bond angle for C18-C22-C20 is observed as 119.39° and 119.68° calculated by DFT/HF methods respectively, which shows a good agreement with the experimental data(119.91°) [16].

The bond angle of C12-N14-C15 is 121.05°/120.24° calculated by DFT/HF methods which is closer to the experimental data (121°).The bond angles of H27-C25-O29 and H28-C25-O29 by DFT/HF methods are 111.49°/111.06° and 111.53°/111.18° which is greater than the experimental finding (109.5°).The dihedral angles are calculated according to the atoms C2-C3-C12-N14 (-178.64°/-178.1°) and C4-C3-C12-N14 (1.22°/1.83°) by DFT/HF methods.

**Vibration analysis:** The vibration analysis is used to find vibrational modes of molecular structures of the compound. The experimental and theoretical FT-IR and FT-Raman spectra of CBMA are shown in Figs. 4 and 5, respectively.

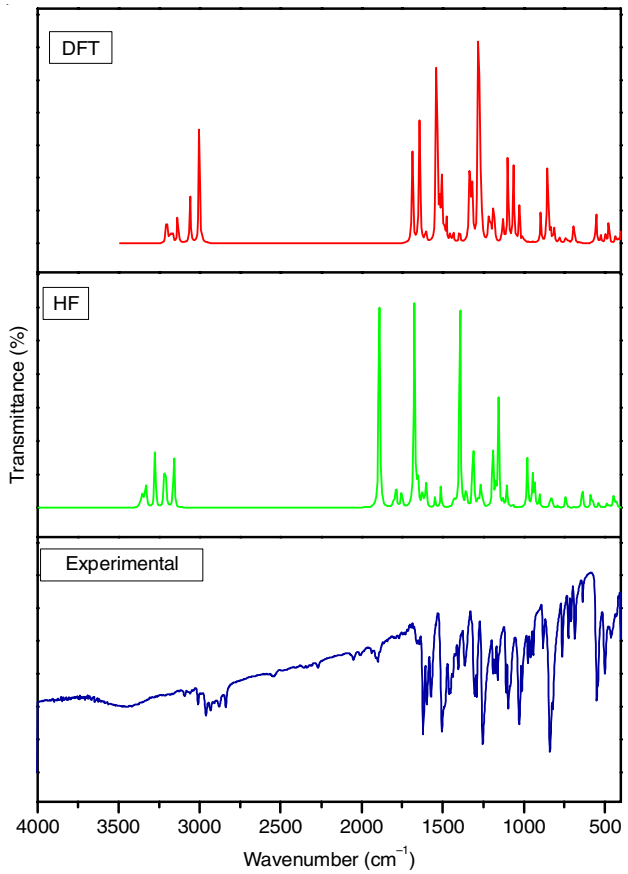


Fig. 4. Comparison of experimental and theoretical HF/B3LYP/6-311G (d,p) FT-IR spectra for CBMA

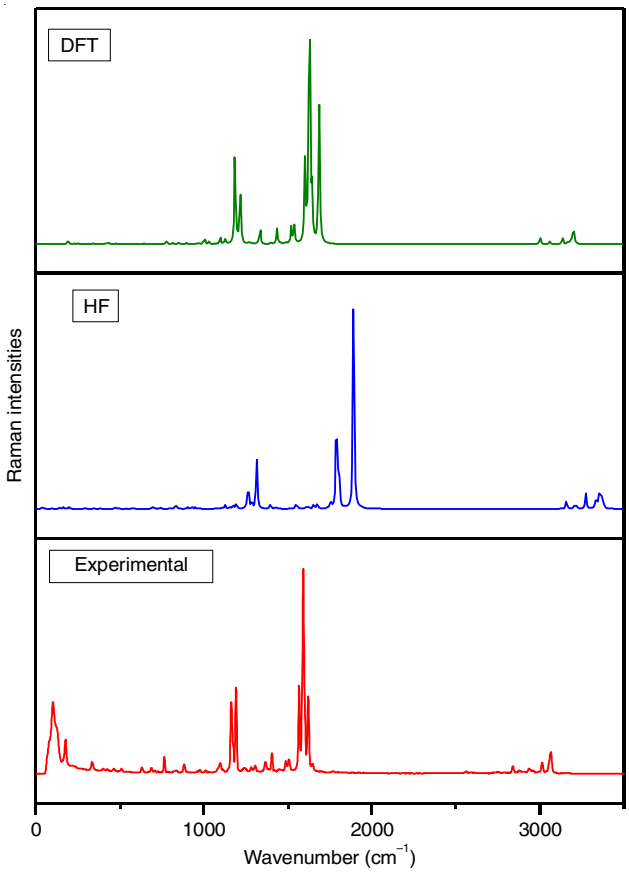


Fig. 5. Comparison of experimental and theoretical HF/B3LYP/6-311G (d,p) FT-Raman spectra for CBMA

The observed and calculated FTIR and FT-Raman wave numbers of vibrational modes of CBMA are depicted in Table-2. In the present study, the scaling factors of 0.9085 and 0.9668 are followed for HF and DFT methods respectively. According to the theoretical calculations, CBMA has a planar structure. The molecule has 29 atoms and 81 normal modes of fundamental vibrations. All the 81 vibrations are distributed as 28 stretching, 27 in plane bending, 26 torsional and 4 out of plane bending vibrations. All the fundamental vibrations are found to be active in both IR and Raman regions.

**C-C vibrations:** The ring stretching vibrations are very important in the spectrum of benzene. Most of the ring vibrations are affected by the substitution to the aromatic ring of benzene derivatives. The six ring carbon atoms undergo skeletal vibration. The C-C stretching modes of the phenyl group are expected in the range from 1625 to 1430 $cm^{-1}$. For the molecule (CBMA), C-C stretching vibration peaks are obtained at 1623, 1577, 1451, 1407 and1362 $cm^{-1}$.

**C-H vibrations:** The aromatic organic compounds and their derivatives are very close to benzene and exhibit multiple

TABLE-2
COMPARISON OF THE EXPERIMENTAL AND CALCULATED VIBRATIONAL SPECTRA OF CBMA

| Mode No. | Experimental wavenumber ($cm^{-1}$) | | Theoretical wavenumbers ($cm^{-1}$) | | | | | | | | Vibrational assignments |
|---|---|---|---|---|---|---|---|---|---|---|---|
| | FT-IR | FT-Raman | HF/6-311G(d,p) | | | | DFT/B3LYP/6-311G(d,p) | | | | |
| | | | Unscaled | Scaled | $^{a}I_{iR}$ | $^{b}I_{RA}$ | Unscaled | Scaled | $^{a}I_{iR}$ | $^{b}I_{RA}$ | |
| 1 | 3062m | 3069w | 3376 | 3067 | 1.74 | 90.67 | 3206 | 3118 | 3.18 | 144.34 | ν(CH) |
| 2 | | | 3366 | 3058 | 5.22 | 113.65 | 3203 | 3096 | 12.26 | 134.97 | ν(NC) |
| 3 | | | 3358 | 3050 | 1.77 | 60.74 | 3202 | 3095 | 4.41 | 122 | ν(CH) |
| 4 | | | 3355 | 3048 | 6.98 | 147.47 | 3198 | 3091 | 8.09 | 140.53 | ν(NC) |
| 5 | | | 3349 | 3042 | 13.06 | 78.91 | 3193 | 3086 | 0.63 | 52.81 | ν(ClC) |
| 6 | 3036m | | 3336 | 3030 | 9.53 | 87.04 | 3183 | 3077 | 4.71 | 87.84 | ν(CH) |
| 7 | | | 3331 | 3026 | 14.23 | 31.2 | 3175 | 3069 | 8.36 | 29.42 | ν(CH) |
| 8 | 3015m | 3016w | 3327 | 3022 | 11.45 | 56.96 | 3165 | 3059 | 7.99 | 53.73 | ν(CH) |
| 9 | | | 3274 | 2974 | 63.93 | 191.56 | 3133 | 3028 | 28.77 | 192.75 | ν(CH) |
| 10 | 2935m | | 3217 | 2922 | 49.37 | 40.35 | 3058 | 2953 | 42.6 | 72.17 | ν(CH) |
| 11 | 2930m | | 3207 | 2913 | 32.89 | 33.64 | 3002 | 2902 | 56.17 | 46.52 | ν(CH) |
| 12 | 2842m | 2845w | 3158 | 2869 | 65.13 | 109.78 | 3000 | 2900 | 64.06 | 150.54 | ν(CH) |
| 13 | 1942m | | 1892 | 1718 | 282.3 | 2183.07 | 1685 | 1629 | 85.88 | 2801.54 | ν(OH) |
| 14 | | | 1802 | 1637 | 8.55 | 369.28 | 1643 | 1588 | 115.54 | 111.86 | ν(CH) |
| 15 | 1623s | 1620m | 1788 | 1624 | 31.12 | 941.69 | 1627 | 1572 | 3.46 | 5833.13 | ν(CC) |
| 16 | | | 1756 | 1595 | 0.7 | 12.51 | 1606 | 1552 | 6.59 | 54.91 | ν(CC) |
| 17 | 1577m | 1591vs | 1753 | 1592 | 23.68 | 51.33 | 1603 | 1549 | 4.64 | 1466.5 | ν(CC) |
| 18 | | 1566s | 1674 | 1520 | 272.01 | 48.07 | 1537 | 1485 | 220.57 | 471.72 | ν(CH) |
| 19 | 1507s | | 1654 | 1502 | 34.85 | 36.82 | 1519 | 1468 | 27.95 | 306.54 | ν(CH) |
| 20 | | | 1627 | 1478 | 21.16 | 13.85 | 1506 | 1456 | 59.15 | 6.69 | ν(CH) |
| 21 | | | 1612 | 1464 | 7.7 | 16.2 | 1491 | 1441 | 8.12 | 22.3 | ν(CH) |
| 22 | 1451m | | 1602 | 1455 | 24.67 | 4.71 | 1477 | 1427 | 20.58 | 8.68 | ν(CH) |
| 23 | | | 1557 | 1414 | 0.25 | 23.75 | 1454 | 1405 | 8.26 | 26.8 | ν(CC) |
| 24 | 1407w | 1404w | 1547 | 1405 | 10.69 | 31.75 | 1435 | 1387 | 8.29 | 295.4 | ν(CC) |
| 25 | 1362w | | 1511 | 1372 | 22.87 | 3.53 | 1396 | 1349 | 12.73 | 37.17 | ν(CC) |
| 26 | | | 1431 | 1300 | 10.61 | 13.33 | 1335 | 1290 | 64.4 | 270.12 | ν(CC) |
| 27 | 1295m | | 1420 | 1290 | 2.02 | 2.94 | 1327 | 1282 | 33.98 | 61.98 | ν(OC) |
| 28 | 1256vs | | 1394 | 1266 | 262.41 | 35.83 | 1319 | 1275 | 7.93 | 6.11 | ν(CC) |
| 29 | | | 1354 | 1230 | 22.97 | 1.61 | 1316 | 1272 | 42.11 | 5.68 | δ(OHC) |
| 30 | | 1192s | 1314 | 1193 | 29.94 | 394.69 | 1277 | 1234 | 276.34 | 26.34 | δ(CCC) |
| 31 | | | 1309 | 1189 | 51.12 | 4.21 | 1265 | 1223 | 41.06 | 29.76 | δ(CCC) |
| 32 | 1164w | 1163m | 1284 | 1166 | 5.51 | 53.38 | 1215 | 1174 | 29 | 1158.2 | δ(CCC) |
| 33 | 1160w | | 1279 | 1161 | 4.97 | 3.34 | 1204 | 1164 | 10.76 | 16.2 | δ(CNC) |
| 34 | | | 1267 | 1151 | 16.05 | 14.23 | 1190 | 1150 | 24.63 | 277.79 | δ(CCC) |
| 35 | | | 1263 | 1147 | 12.8 | 185.96 | 1183 | 1143 | 16.22 | 1427.75 | δ(NCC) |
| 36 | | | 1251 | 1136 | 5.09 | 13.42 | 1170 | 1131 | 0.72 | 2.93 | δ(ClCC) |
| 37 | 1091m | 1099w | 1192 | 1083 | 77.86 | 43.42 | 1128 | 1090 | 17.66 | 11.31 | δ(HCC) |
| 38 | | | 1175 | 1067 | 17.46 | 18.3 | 1126 | 1088 | 5.42 | 66.68 | δ(HCC) |
| 39 | | | 1170 | 1062 | 10.14 | 9.17 | 1097 | 1060 | 92.91 | 127.9 | δ(HCC) |
| 40 | 1033s | | 1154 | 1048 | 118.2 | 11.18 | 1062 | 1026 | 78.01 | 8.76 | δ(HCC) |
| 41 | | | 1127 | 1023 | 1.22 | 26.6 | 1027 | 1027 | 34.18 | 41.32 | δ(HCH) |
| 42 | | | 1111 | 1009 | 0.31 | 2.11 | 1021 | 987 | 0.24 | 0.51 | δ(CCC) |
| 43 | | | 1103 | 1002 | 27.27 | 6.25 | 1005 | 971 | 5.34 | 86.95 | δ(HCH) |
| 44 | | | 1101 | 1000 | 2.13 | 1.11 | 993 | 960 | 1.23 | 39.13 | δ(CCC) |

| | | | | | | | | | | | |
|---|---|---|---|---|---|---|---|---|---|---|---|
| 45 | | | 1091 | 991 | 0.48 | 2.25 | 972 | 939 | 0.65 | 7.57 | δ(CCC) |
| 46 | 974w | | 1075 | 976 | 0.36 | 2.32 | 961 | 929 | 0.34 | 22.35 | δ(HCC) |
| 47 | | | 1067 | 969 | 3.37 | 0.65 | 942 | 910 | 0.96 | 6.22 | δ(HCC) |
| 48 | | 885w | 978 | 888 | 63.72 | 3.31 | 896 | 866 | 26.69 | 26.14 | δ(HCC) |
| 49 | | | 946 | 859 | 29.84 | 10.76 | 855 | 826 | 61.03 | 5.17 | δ(HCC) |
| 50 | | | 943 | 856 | 11.15 | 0.4 | 850 | 821 | 21.31 | 15.79 | δ(HCN) |
| 51 | | | 931 | 845 | 24.06 | 0.45 | 847 | 818 | 10.24 | 7.49 | δ(CCC) |
| 52 | 837vs | | 928 | 843 | 1.11 | 10.95 | 832 | 804 | 10.14 | 4.35 | δ(CCO) |
| 53 | | | 903 | 820 | 14.22 | 10.31 | 813 | 786 | 14.58 | 32.53 | δ(CCC) |
| 54 | 762w | 766w | 836 | 759 | 12.15 | 30.22 | 778 | 752 | 5.24 | 55.46 | δ(COH) |
| 55 | 725w | | 826 | 750 | 8.33 | 8.55 | 739 | 714 | 5.77 | 3.22 | δ(CCN) |
| 56 | | | 791 | 718 | 2.45 | 1.9 | 724 | 699 | 2.65 | 1.9 | τ(CCCC) |
| 57 | 685w | | 740 | 672 | 13.65 | 6.89 | 690 | 667 | 19.94 | 7.97 | τ(CNCC) |
| 58 | 636w | | 703 | 638 | 0.04 | 5.33 | 654 | 632 | 0.73 | 4.76 | τ(CCCC) |
| 59 | | | 691 | 627 | 0.53 | 11.78 | 644 | 622 | 0.3 | 12.7 | τ(HCCC) |
| 60 | | | 640 | 581 | 27.72 | 0.25 | 562 | 543 | 5.87 | 4.17 | τ(HCCO) |
| 61 | 548m | | 586 | 532 | 15.87 | 1.58 | 552 | 533 | 24.66 | 2.65 | τ(HCCC) |
| 62 | | | 575 | 522 | 6.79 | 4.12 | 523 | 505 | 7.07 | 1.95 | τ(HCCC) |
| 63 | 499m | | 537 | 487 | 6.67 | 1.11 | 495 | 478 | 8.34 | 3.58 | τ(HCHO) |
| 64 | 453w | | 488 | 443 | 5.11 | 3.62 | 475 | 459 | 17.68 | 11.76 | τ(CCCC) |
| 65 | | | 472 | 428 | 3.07 | 9.18 | 432 | 417 | 6.2 | 25.17 | τ(HCHO) |
| 66 | | | 460 | 417 | 0.49 | 0.44 | 423 | 408 | 0.06 | 0.6 | τ(CCCN) |
| 67 | | | 445 | 404 | 18.49 | 0.46 | 415 | 401 | 4.7 | 12.63 | τ(CCCC) |
| 68 | 399w | | 429 | 389 | 8.64 | 0.65 | 395 | 381 | 18.07 | 10.96 | τ(HCCO) |
| 69 | | 340w | 383 | 347 | 1.58 | 3.59 | 340 | 328 | 6.45 | 12.34 | τ(HCCC) |
| 70 | | | 344 | 312 | 5.99 | 2.6 | 326 | 315 | 2.05 | 5.8 | τ(HCCC) |
| 71 | | | 296 | 268 | 6.37 | 5.23 | 262 | 253 | 1.28 | 0.12 | τ(HCCC) |
| 72 | | | 262 | 238 | 0.2 | 0.97 | 250 | 241 | 5.62 | 18.26 | τ(HCNC) |
| 73 | | 178m | 196 | 178 | 5.23 | 10.6 | 232 | 224 | 1.26 | 9.06 | τ(CCCC) |
| 74 | | | 179 | 162 | 0.58 | 0.31 | 192 | 185 | 10.74 | 52.69 | τ(CCOC) |
| 75 | | | 160 | 145 | 0.97 | 9.46 | 185 | 178 | 0.37 | 2.8 | τ(CCCO) |
| 76 | | | 140 | 127 | 3.59 | 4.21 | 138 | 133 | 0.41 | 1.99 | τ(COHC) |
| 77 | | 104s | 95 | 86 | 1.33 | 2.34 | 103 | 99 | 0.8 | 3.7 | τ(CCNC) |
| 78 | | | 53 | 48 | 2.4 | 1.99 | 81 | 78 | 1.68 | 3.3 | γ(ClCCC) |
| 79 | | | 40 | 36 | 0.46 | 3.4 | 45 | 43 | 0.44 | 2.1 | γ(CCCC) |
| 80 | | | 37 | 33 | 1.03 | 3.85 | 38 | 36 | 0.78 | 9.9 | γ(NCCC) |
| 81 | | | 31 | 28 | 1.52 | 1.85 | 30 | 29 | 0.21 | 1.2 | γ(COCC) |

ν = Stretching; δ = in-plane bending; γ = out-of-plane bending: torsion; vs: very strong; s: strong; w: weak; m: medium.
[a]IR intensity (K mmol$^{-1}$); [b]Raman intensity (Arb. units).

weak bands in the region 3100-3000 cm$^{-1}$ due to C-H stretching vibrations [26]. In this region, the bands are not affected much by the nature of substituent. The C-H stretching modes usually appear with strong Raman intensity and are highly polarized. The bands appear in the whole range of the spectrum [27].

In the present investigation, the FT-IR and FT-Raman spectral wave numbers are assigned to the C-H stretching modes of the aromatic group of CBMA. The theoretically computed wavenumbers by HF/6-311G(d,p) method are found to be 3067, 3050, 3030, 3026, 3022, 2974, 2922, 2913 and 2869 cm$^{-1}$ whereas DFT/B3LYP/6-311G(d, p) method results the wave numbers at 3118, 3095, 3077, 3069, 3059, 3028, 2953, 2902 and 2900 cm$^{-1}$ that fall within the recorded spectral range.

The in-plane aromatic C-H bending vibrations occur in the region 1400-1000 cm$^{-1}$. The C-H in plane bending vibrations are at 1478, 1464 and 1455 cm$^{-1}$computed by HF and at 1456, 1441 and 1427 cm$^{-1}$ by B3LYP method, which shows an agreement with the medium FT-IR band at 1451 cm$^{1}$.

**Methoxy group vibrations:** If the $CH_3$ group is directly attached to oxygen atom, the C-H bending and stretching bands would shift their positions due to electronic effects [28]. This causes the O-$CH_3$ stretching bands to be spread over a larger region than that of the C-$CH_3$ group. The medium band is observed at 1295 cm$^{-1}$ in the FTIR spectrum. The mode Nos.6,11 and 14 show the C-H bonds.

**C-N and C=N vibrations:** The C-N stretching vibration [29] coupled with δ(NH) is strongly active in the region [30] 1275 ± 55 cm$^{-1}$. The C=N stretching skeletal bands are expected in the range 1672-1566 cm$^{-1}$ [31]. For the molecule CBMA, the FTIR spectrum shows the C-N band at 1160 and C=N band at 725 cm$^{-1}$.

**C-Cl vibrations:** Mooney [32] assigned vibrations of C-X group (X = F, Cl, Br and I) in the frequency range of 1129-480 cm$^{-1}$. The C-Cl stretching mode is reported at 738 cm$^{-1}$ for dichloromethane and scissoring mode δ(C-Cl) at 284 cm$^{-1}$ [33-35] reported C-Cl stretching mode at 890 cm$^{-1}$. For the CBMA, the C-Cl stretching frequency appears at 548 cm$^{-1}$ in the FTIR spectrum. HF method shows the C-Cl vibrations at 3050, 1136, 532, 268 and 48 cm$^{-1}$. DFT/B3LYP method shows those vibrations at 3095, 1130, 533, 253 and 78 cm$^{-1}$.

**NBO analysis:** The natural bond orbital (NBO) analysis is a method to study intra- and intermolecular bonding and interaction among bonds. It investigates charge transfer or conjugative interaction in molecular systems [36]. The NBO analysis was done by examining all possible interactions between 'filled' (donor) Lewis-type NBOs and 'empty' (acceptor) non-Lewis NBOs and estimating their energies by second order perturbation theory. A lone pair donor → anti-bonding acceptor orbital interaction will weaken the bond which is associated with the anti-bonding orbital. Conversely, an interaction with a bonding pair as the acceptor can strengthen the bond [37]. The second order Fock-matrix evaluates the donor-acceptor interactions in the NBO basis. However, the strengths of these delocalization interactions ($E_2$) are estimated by second order perturbation theory by using the following equation:

$$E_2 = \Delta E_{ij} = q_i \frac{F(i,j)_2}{\varepsilon_j - \varepsilon_i} \quad (2)$$

where $q_i$ is the donor orbital occupancy; $\varepsilon_i$ and $\varepsilon_j$ are the diagonal elements; $F_{ij}$ is the off diagonal NBO Fock matrix element. For the larger $E_2$ value, the donation tendency from electron donors to electron acceptors increases with the extent of conjugation of the whole system. The intramolecular interactions are formed by the orbital overlap between σ(C-C) and σ*(C-C); π(C-C) and π*(C-C) and LP(1),LP(2) and LP(3) bond orbital which results intramolecular charge transfer (ICT) making stabilization of the system.

In the CBMA molecule, the π electron delocalization is maximum around C2-C3, C4-C5, C16-C18 and C20-C22 distributed to π* antibonding of C1-C6, C4-C5, C20-C22 and C15-C17 with a stabilization energy of 21.76,19.57,21.98,21.55 and 21.48 KJ/mol as shown in Table-3. The electron density transfer observed from the interaction LP (3)Cl11 → π*(C1-C6) results in stabilization energy of 12.57 KJ/mol. The charge transfer from the lone electron pair of LP (2)O29 atom to π*(C20-C22) and π*(C25-H27) antibonding orbital results in stabilization energy of 30.64 KJ/mol,5.64 KJ/mol. π*(C1-C6) and π*(C20-C22) of the NBO conjugated with π*(C2-C3), π*(C4-C5) and π*(C5AC6) leads to an enormous stabilization energy of 213.88, 136.12 and 211.16 KJ/mol respectively. This strong stabilization represents a larger delocalization.

**Non-linear optical properties-first order hyperpolarizability:** Quantum chemical calculations explain the relationship between the electronic structure of the systems and its NLO response [38]. The computational methods help to determine molecular NLO properties in an inexpensive way to explain the molecules properties. The NLO activity explains optical modulation, optical switching, frequency shifting and optical logic for the communication, signal processing and optical interconnections [22,39].

The non-linear optical properties are analyzed by the polarization of the molecule in an external radiation field. For the weak polarization condition, dipolar interaction is demonstrated by Taylor series. The first static hyperpolarizability ($\beta_0$) and its related properties such as static polarizability (α), hyperpolarizability (β) and electric dipole moment (μ) have been calculated using HF/B3LYP/6-311G(d,p) levels. The first hyperpolarizability is a third rank tensor in the presence

TABLE-3
SECOND ORDER PERTURBATION ANALYSIS OF FOCK MATRIX IN NBO BASIS FOR CBMA

| Donor(i) | Ed(i)(e) | Acceptor(j) | ED(j)(e) | E(2)[a] ( KJ/mol) | E(j)-E(i)[b] (a.u) | F(ij)[c] (a.u) |
|---|---|---|---|---|---|---|
| π(C1-C2) | 1.969 | π*(C6-Cl11) | 0.034 | 5.37 | 0.84 | 0.060 |
| π(C1-C6) | 1.677 | π*(C2-C3) | 0.374 | 18.84 | 0.30 | 0.068 |
| | | π*(C4-C5) | 0.28 | 17.75 | 0.31 | 0.067 |
| π(C2-C3) | 1.631 | π*(C1-C6) | 0.388 | 21.76 | 0.27 | 0.068 |
| | | π*(C4-C5) | 0.28 | 19.57 | 0.29 | 0.068 |
| | | π*(C12-N14) | 0.154 | 17.63 | 0.29 | 0.068 |
| π(C4-C5) | 1.668 | π*(C1-C6) | 0.388 | 21.98 | 0.27 | 0.070 |
| | | π*(C2-C3) | 0.374 | 19.02 | 0.29 | 0.067 |
| π(C12-N14) | 1.908 | π*(C15-C17) | 0.388 | 10.42 | 0.36 | 0.059 |
| π(C15-C17) | 1.654 | π*(C16-C18) | 0.301 | 19.6 | 0.29 | 0.068 |
| | | π*(C20-C22) | 0.395 | 18.42 | 0.28 | 0.065 |
| π(C16-C18) | 1.713 | π*(C15-C17) | 0.388 | 17.72 | 0.29 | 0.065 |
| | | π*(C20-C22) | 0.395 | 21.55 | 0.28 | 0.071 |
| π(C20-C22) | 1.658 | π*(C15-C17) | 0.388 | 21.48 | 0.29 | 0.072 |
| | | π*(C16-C18) | 0.301 | 16.23 | 0.30 | 0.063 |
| LP(3)Cl11 | 1.924 | π*(C1-C6) | 0.388 | 12.57 | 0.33 | 0.063 |
| LP(1)N14 | 1.891 | π*(C12-H13) | 0.041 | 12.62 | 0.73 | 0.087 |
| | | π*(C15-C17) | 0.033 | 7.16 | 0.91 | 0.073 |
| LP(1)O29 | 1.962 | π*(C20-C22) | 0.03 | 7.22 | 1.10 | 0.080 |
| LP(2)O29 | 1.838 | π*(C20-C22) | 0.395 | 30.64 | 0.34 | 0.097 |
| | | π*(C25-H27) | 0.019 | 5.64 | 0.69 | 0.058 |
| | | π*(C25-H28) | 0.019 | 5.78 | 0.69 | 0.058 |
| π*(C1-C6) | 0.388 | π*(C2-C3) | 0.374 | 213.88 | 0.02 | 0.085 |
| | | π*(C4-C5) | 0.28 | 136.12 | 0.02 | 0.080 |
| π*(C20-C22) | 0.395 | π*(C16-C18) | 0.301 | 211.16 | 0.01 | 0.082 |

$E_D$ means electron density; [a]E(2) means energy of hyper conjugative interactions; [b]Energy difference between donor and acceptor i and j NBO orbitals; [c]F(i, j) is the Fock matrix element between i and j NBO orbitals.

of an applied electric field. The 27 components of the 3D matrix which is given in the lower tetrahedral format can be reduced to 10 components because of the Kleinman symmetry [22].

The total static dipole moment (μ), the mean polarizability ($\alpha_0$), the anisotropy of the polarizability ($\Delta\alpha$) and the mean first hyperpolarizability ($\beta_0$) using the x, y and z components are defined as:

$$\mu = (\mu_x^2 + \mu_y^2 + \mu_z^2)^{1/2} \quad (3)$$

$$\alpha_0 = (\alpha_{xx} + \alpha_{yy} + \alpha_{zz})/3 \quad (4)$$

$$\Delta\alpha = 2^{-1/2}[(\alpha_{xx} - \alpha_{yy})^2 + (\alpha_{yy} - \alpha_{zz})^2 + (\alpha_{zz} - \alpha_{xx})^2 + 6\alpha^2_{xz} + 6\alpha^2_{xy} + 6\alpha^2_{yz}]^{1/2} \quad (5)$$

$$\beta = (\beta_x^2 + \beta_y^2 + \beta_z^2)^{1/2} \quad (6)$$

Since the values are calculated in atomic units (a.u.), the reported values have been converted into electrostatic units (esu) (For α, 1 a.u. = $0.1482 \times 10^{-24}$ esu; for β, 1 a.u. = $8.639 \times 10^{-33}$ esu) [40]. The mean polarizability ($\alpha_0$), total polarizability ($\Delta\alpha$), total molecular dipole moment (μ) and first order hyperpolarizability (β), of the CBMA in different media are shown in Table-4. Total dipole moment of CBMA molecule is three times greater than that of urea and first order hyperpolarizability approximately 70 times greater than that of urea (μ and β of urea are 1.3732 Debye and $0.3728 \times 10^{-30}$ esu respectively [41]). This result confirms the good non-linearity of the CBMA molecule.

## Electronic properties

**UV-visible spectral analysis:** Ultraviolet spectral analysis of CBMA has been investigated in gas, methanol, ethanol, benzene, dichloroethane and dimethyl sulfoxide by theoretical calculation. TD-DFT/B3LYP/6-311G(d,p) calculations have been used to determine the low-level excited states of CBMA. The theoretical UV spectra of CBMA are shown in Fig. 6. Calculations regarding the excitation energies, oscillator strength (f) and wavelength (λ) have been carried out and the results were compared (Table-5) with the measured experimental wavelengths.

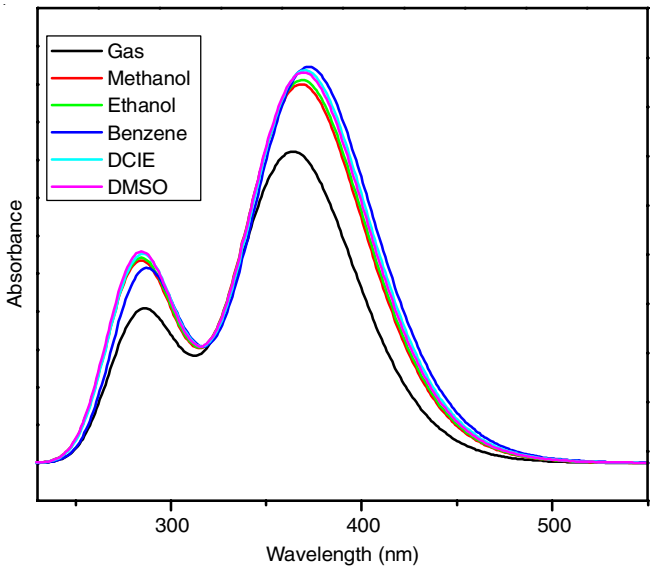


Fig. 6. Theoretical UV spectra of CBMA in different solvents

Based on the Frank-Condon principle, the maximum absorption peak ($\lambda_{max}$) in a UV-visible spectrum corresponds to vertical excitation. The calculations performed for ethanol and methanol are very close to each other while comparing

TABLE-4
ELECTRIC DIPOLE MOMENT, POLARIZABILITY AND FIRST ORDER HYPERPOLARIZABILITY OF CBMA BY DFT/B3LYP/6-311G(d,p) METHOD

| | Gas | Methanol | Ethanol | Benzene | Dichloroethane | Dimethyl sulfoxide |
|---|---|---|---|---|---|---|
| Dipole moment (μ) | 3.514 | 4.491 | 4.472 | 3.921 | 4.362 | 4.51 |
| Polarizability | | | | | | |
| $\alpha_{xx}$ | 384.015 | 485.8343 | 484.3936 | 433.7619 | 475.861 | 487.2472 |
| $\alpha_{xy}$ | -1.6206 | -6.4663 | -6.3573 | -3.4004 | -5.745 | -6.5749 |
| $\alpha_{yy}$ | 158.416 | 222.1806 | 220.8531 | 183.4727 | 213.352 | 223.5006 |
| $\alpha_{xz}$ | 0.2055 | 0.6699 | 0.6614 | 0.3881 | 0.6111 | 0.6782 |
| $\alpha_{yz}$ | 2.6508 | 4.2248 | 4.1874 | 3.218 | 3.9801 | 4.2623 |
| $\alpha_{zz}$ | 84.5107 | 109.1256 | 108.5103 | 93.1333 | 105.132 | 109.7429 |
| $\alpha_0$ | 208.98 | 272.3802 | 271.25 | 236.78 | 264.78 | 273.49 |
| Δα (a.u) | 270.245 | 334.8184 | 334.143 | 305.64 | 330.201 | 335.417 |
| Δα (esu × $10^{-24}$) | 40.05 | 49.61 | 49.55 | 45.29 | 48.93 | 49.71 |
| Hyperpolarizability | | | | | | |
| $\beta_{xxx}$ | 3086.55 | 6644.7279 | 6586.306 | 4660.148 | 6243.6 | 6702.163 |
| $\beta_{xyy}$ | -70.51 | -143.8972 | -142.271 | -98.0427 | -133.139 | -145.517 |
| $\beta_{xzz}$ | -46.26 | -72.7867 | -72.1461 | -56.0401 | -68.6366 | -73.43 |
| $\beta_{yyy}$ | -50.72 | -86.6843 | -85.9062 | -63.6516 | -81.4195 | -87.4515 |
| $\beta_{yzz}$ | -46.33 | 81.9285 | -81.0185 | -58.653 | -76.047 | -82.8429 |
| $\beta_{xxy}$ | -179.03 | -443.5372 | -437.653 | -276.9125 | -404.536 | -449.394 |
| $\beta_{zzz}$ | 32.42 | 55.31029 | 54.734 | 40.478 | 51.5829 | 55.8891 |
| $\beta_{xxz}$ | -163.55 | -366.509 | -362.202 | -242.7718 | -337.998 | -370.8 |
| $\beta_{yyz}$ | -40 | -80.1164 | -79.1391 | -54.2357 | -73.7446 | -81.095 |
| $\beta_{xyz}$ | 57.62 | 120.1067 | 118.8923 | 82.6721 | 111.909 | 121.3073 |
| β (a.u) | 2987.49 | 6455.528 | 6412.16 | 4530.987 | 6078.59 | 6524.73 |
| β (esu × $10^{-30}$) | 25.8 | 55.77 | 55.39 | 37.57 | 52.5 | 56.36 |

TABLE-5
CALCULATED WAVELENGTH (λ, nm), EXCITATION ENERGIES (E, eV) AND OSCILLATOR STRENGTH

| | E (eV) | λ (nm) | (f) |
|---|---|---|---|
| Gas | 3.4040 | 364.19 | 0.5066 |
| | 4.3380 | 285.77 | 0.2467 |
| Methanol | 3.3650 | 368.44 | 0.6168 |
| | 4.3490 | 285.08 | 0.2928 |
| Ethanol | 3.3602 | 368.97 | 0.6238 |
| | 4.3465 | 285.25 | 0.2968 |
| Benzene | 3.3296 | 372.37 | 0.6449 |
| | 4.3176 | 287.16 | 0.3139 |
| Dichloroethane | 3.3468 | 370.46 | 0.6394 |
| | 4.3376 | 285.84 | 0.3059 |
| Dimethyl sufloxide | 3.3546 | 369.59 | 0.6360 |
| | 4.3452 | 285.33 | 0.3031 |

with other solvents. The absorption maxima values of gas phase are smaller than that in the organic solvents. However, polar solvents such as methanol, ethanol *etc*., may stabilize or destabilize the molecular orbital of a molecule either in the ground state or in excited state. The electronic absorption spectra of CBMA showed two bands at 245 and 365 nm. These excitations correspond to π-π* transition, which is more polar than the ground state.

**Frontier molecular orbital analysis:** Many organic molecules, containing conjugated π-electrons with large first hyperpolarizabilities are analyzed by means of vibrational spectroscopy [42,43]. In most of the cases, the strongest bands in the Raman spectrum are weak in the IR spectrum and *vice versa* even in the absence of inversion symmetry. The intramolecular charge transfer from the donor to accepter group can induce large variations in dipole moment and the molecular polarizability. The important frontier molecular orbital are the highest occupied molecular orbital (HOMO) and lowest occupied molecular orbital (LUMO). These orbitals determine the way the molecule interacts with other species. The frontier orbital gap helps to analyze the chemical reactivity and kinetic stability of the molecule. A molecule with a small frontier orbital gap is more polarizable with a high chemical reactivity and low kinetic stability. It is also termed as a soft molecule [44]. The frontier molecular orbitals show an important role in the electronic, optical properties and chemical reactions [45,46]. The conjugated molecules are explained by HOMO-LUMO separation by the intramolecular charge transfer from the efficient electron-donor groups to the electron-acceptor groups through π-conjugated path [47].

The HOMO has an ability to donate an electron whereas LUMO is an electron acceptor. The HOMO and LUMO energies calculated by B3LYP/6-311G(d,p) method are shown in Table-6. This electronic absorption corresponds to the transition from the ground state to the first excited state depicted by one electron excitation from the HOMO to the LUMO. The energy of the HOMO and LUMO is directly related to the ionization potential and electron affinity respectively. The energy difference between HOMO and LUMO orbital is called as energy gap which is an important for structure stability [48] and is given in Table-6. The plots of HOMOs and LUMOs are shown in Fig. 7(a-f). The frontier energy gap of CBMA in gas, methanol, ethanol, benzene, dichloroethane and dimethyl sulfoxide are found to be 0.1419 eV, 0.1424 eV, 0.1423 eV, 0.142 eV, 0.142 eV and 0.1423 eV respectively obtained by DFT method using 6-311G(d,p) basis set. The HOMO is located whole of the molecules except some -C-H groups and LUMO is contributed by the whole of the molecules except methyl group.

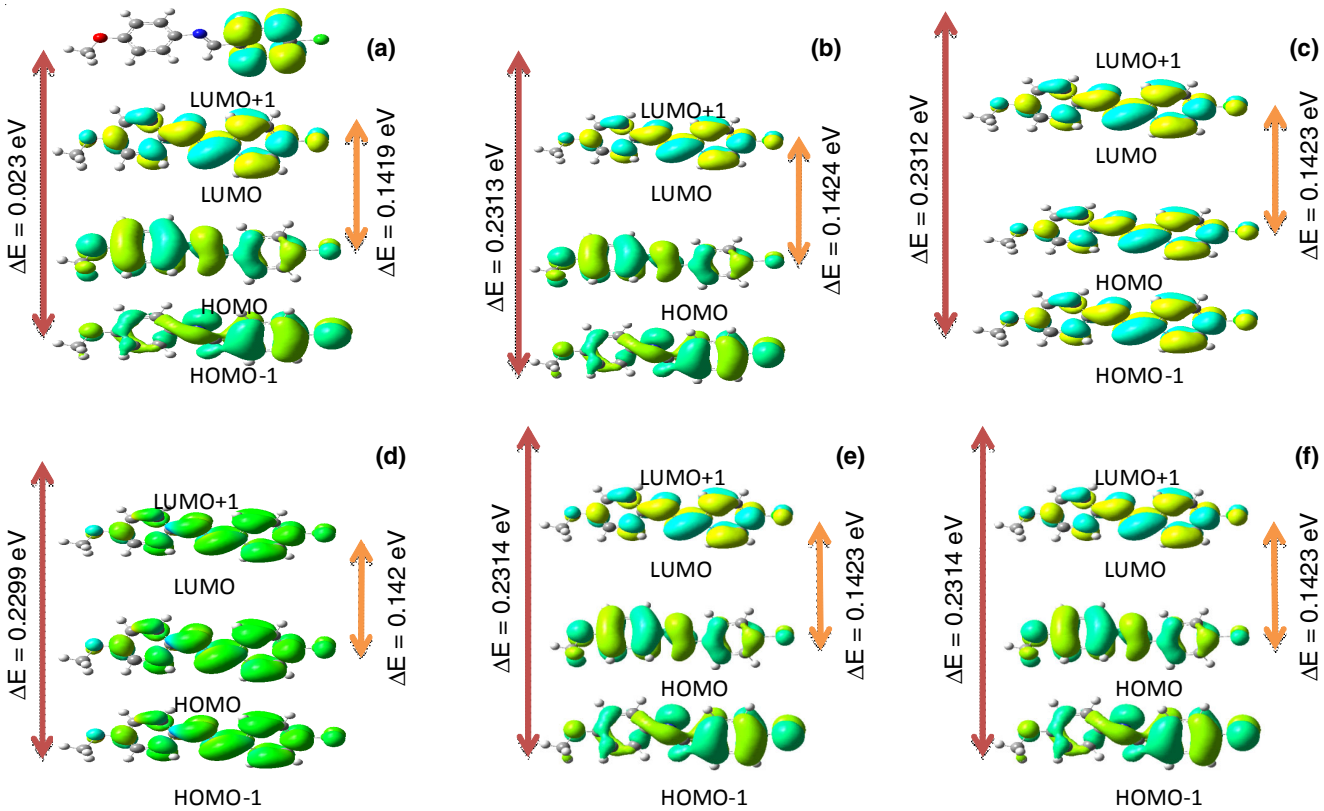


Fig. 7. Frontier and second frontier molecular orbitals of CBMA in (a) gas, (b) methanol, (c) ethanol, (d) benzene, (e) dichloroethane and (f) dimethyl sulfoxide

TABLE-6
CALCULATED ENERGY VALUES OF CBMA MOLECULES BY THE DFT/B3LYP METHOD USING 6-311G(d,p) BASIS SET

| | Gas | Methanol | Ethanol | Benzene | DClE | DMSO |
|---|---|---|---|---|---|---|
| $E_{HOMO}$ | -0.2127 | -0.2163 | -0.2162 | -0.2138 | -0.216 | -0.2164 |
| $E_{LUMO}$ | -0.0708 | -0.0739 | -0.0739 | -0.0718 | -0.074 | -0.0741 |
| $E_{HOMO} - E_{LUMO}$ | 0.1419 | 0.1424 | 0.1423 | 0.1420 | 0.142 | 0.1423 |
| $E_{HOMO-1}$ | -0.2560 | -0.2602 | -0.2601 | -0.2576 | -0.260 | -0.2603 |
| $E_{LUMO+1}$ | -0.0273 | -0.0289 | -0.0289 | -0.0277 | -0.029 | -0.0289 |
| $E_{HOMO-1} - E_{LUMO+1}$ | 0.2300 | 0.2313 | 0.2312 | 0.2299 | 0.231 | 0.2314 |
| $E_{HOMO-2}$ | -0.2621 | -0.2663 | -0.2662 | -0.2634 | -0.266 | -0.2664 |
| $E_{LUMO+2}$ | -0.0156 | -0.0192 | -0.0191 | -0.0167 | -0.019 | -0.0193 |
| $E_{HOMO-2} - E_{LUMO+2}$ | 0.2470 | 0.2470 | 0.2470 | 0.2470 | 0.247 | 0.2470 |

**Electrostatic potential, total electron density and molecular electrostatic potential:** The molecular electrostatic potential surface is a visual method of mapping electrostatic potential onto the iso-electron density surface which simultaneously displays molecular electrostatic potential (electron + nuclei) distribution, dipole moments, size and shape [49]. Fig. 8 shows the electrostatic potential (ESP), the total electron density (TED) and molecular electrostatic potential (MEP) surfaces of the CBMA molecule by using B3LYP method. The colour scheme of electrostatic potential (Fig. 8a) shows the negative electrostatic potentials in nitrogen atoms (red colour) and slightly electron rich region in oxygen atom (yellow colour). Green areas cover the electrostatic potentials of the molecule which are close to zero (C-C and C-H bonds). The total electron density (TED) plots for CBMA show a uniform distribution (Fig. 8b) computed at 0.020 a.u. iso-density surface. The colour code of these maps is represented in the range between -4.037 e-4 (deepest red) and +4.037 e-4 (deepest blue) in the compound.

The molecular electrostatic potential V(r) is related to the electronic density, which helps to determine sites for electrophilic attack and nucleophilic reactions. Molecular electrostatic potential values are calculated using the equation [50]:

$$V(r) = \Sigma Z_A / |R_A - r| - \int \rho(r^1) / |r^1 - r| d^3 r^1 \quad (7)$$

where $Z_A$ is the charge of nucleus A located at $R_A$, $\rho(r^1)$ is the electronic density function of the molecule and $r^1$ is the dummy integration variable. The colour code of these maps is in the range between -3.295 e-2 (deepest red) and +3.295 e-2 (deepest blue) in the compound (Fig. 8c). The maximum positive region is localized around the hydrogen atoms, indicating nucleophilic attack (blue colour) and the maximum negative region is localized on nitrogen atoms indicating electrophilic attack (red colour).

**Global reactivity descriptors:** The energy gap between HOMO and LUMO is used to calculate global chemical reactivity descriptors of molecules such as hardness (η), chemical potential (μ), softness (S), electro negativity (χ) and electrophilicity index (ω) [51,52]. Those descriptors are calculated on the basis of $E_{HOMO}$ and $E_{LUMO}$ using the below equations.

Using Koopman's theorem [53]:

The hardness of the molecule is

$$\eta = (I - A)/2 \quad (8)$$

The chemical potential of the molecule is

$$\mu = -(I + A)/2 \quad (9)$$

The softness of the molecule is

$$S = 1/2\eta \quad (10)$$

The electronegativity of the molecule is

$$\chi = (I + A)/2 \quad (11)$$

The electrophilicity index of the molecule is

$$\omega = \mu^2/2\eta \quad (12)$$

where I is the ionization potential and A is the electron affinity of the molecule. I and A can be expressed through HOMO and LUMO orbital energies as $I = -E_{HOMO}$ and $A = -E_{LUMO}$. The ionization potential, electron affinity, hardness, softness, chemical potential, electro negativity and electrophilicity index of the title molecule calculated by DFT/B3LYP level of calculation in gas/methanol/ethanol/benzene/dichloroethane/dimethyl sulfoxide environments are shown in Table-7. By considering the chemical hardness, large HOMO-LUMO gap represents a hard molecule and small HOMO-LUMO gap represents a soft molecule. The value of energy gap between the HOMO and LUMO in different environments is small which concludes that CBMA is soft molecule, which is evidenced from Table-7. The chemical softness is found to be 7.042 (DFT-Gas), 7.022 (methanol), 7.032 (ethanol), 7.042 (benzene), 7.032 (dichloroethane) and 7.032 (dimethyl sulfoxide), which is greater than that of chemical hardness.

**Mulliken charge analysis:** Atomic charge plays a significant role in the application of quantum mechanical calculations to

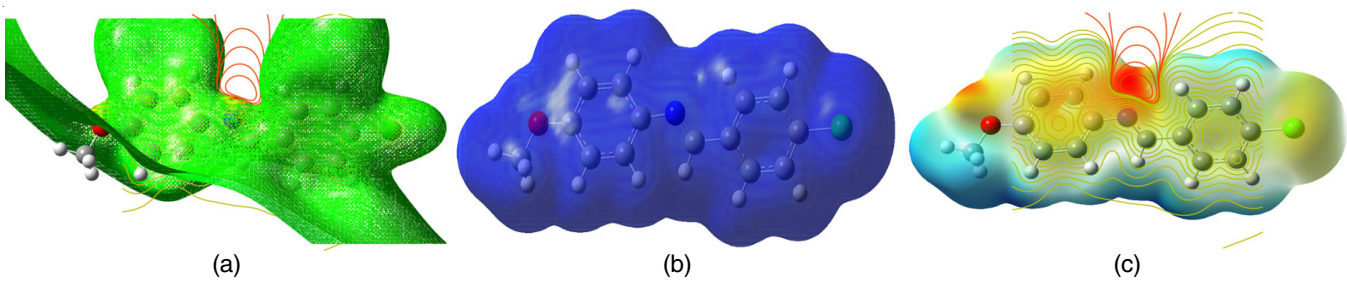


Fig. 8. (a) Electrostatic potential (ESP), (b) Electron density (ED) and (c) Molecular electrostatic potential map (MEP) of CBMA

TABLE-7
GLOBAL CHEMICAL REACTIVITY DESCRIPTORS OF CBMA IN DIFFERENT MEDIA

| | Gas | Methanol | Ethanol | Benzene | DClE | DMSO |
|---|---|---|---|---|---|---|
| Ionization potential (I) | 0.2127 | 0.2163 | 0.2162 | 0.2138 | 0.2157 | 0.2164 |
| Electron affinity (A) | 0.0708 | 0.0739 | 0.0739 | 0.0718 | 0.0735 | 0.0741 |
| Electro negativity (χ) | 0.1417 | 0.1451 | 0.1451 | 0.1428 | 0.1446 | 0.1452 |
| Chemical potential (μ) | -0.1417 | -0.1417 | -0.1451 | -0.1428 | -0.1446 | -0.1452 |
| Chemical hardness (η) | 0.071 | 0.0712 | 0.0711 | 0.071 | 0.0711 | 0.0711 |
| Softness (S) | 7.042 | 7.022 | 7.032 | 7.042 | 7.032 | 7.032 |
| Electrophilicity index (ω) | 0.1414 | 0.141 | 0.1481 | 0.1436 | 0.147 | 0.1482 |

molecular systems. Mulliken atomic charges are calculated by analyzing the electron population of each atom as defined by the basis function [54]. In Fig. 9, the Mulliken atomic charges of CBMA calculated by DFT/B3LYP method using 6-311G(d,p) basis set are shown. The results are shown in Table-8. The magnitudes of the carbon atomic charges are reported to be either positive or negative, which are changing from 0.175 to -0.238. All the hydrogen atoms have a positive charge, whereas oxygen, nitrogen and chlorine have negative charges. The C22 has the maximum positive charge than other atoms since it is an acceptor atom and the atom O29 has a maximum negative charge since it is a donor.

**Thermodynamic properties:** On the basis of vibration analysis, the statistical thermodynamic functions such as heat capacity (C), enthalpy changes (H) and entropy changes (S) for CBMA molecule were obtained from the theoretical harmonic frequencies [55]. Table-9 showed that these thermodynamic parameter values are increasing with temperature ranging from 100 to 700 K. The correlation equations between heat capacity,

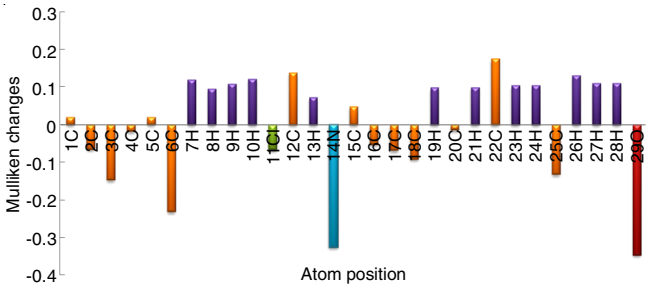


Fig. 9. Histogram of calculated Mulliken charges for CBMA

enthalpy and entropy changes with temperatures were fitted by quadratic formulae and the corresponding fitting factors ($R^2$) for these thermodynamic properties are 0.9999, 0.9998 and 1.0000 respectively. The corresponding fitting equations are given below and the correlation graphs of those are shown in Fig. 10(a-c).

$$C = 2.708 + 0.217\ T - 5 \times 10^{-9}\ T^2 \quad (R^2 = 0.9999) \qquad (13)$$

$$H = 0.016\ T + 5 \times 10^{-6}\ T^2 \quad (R^2 = 0.9998) \qquad (14)$$

TABLE-8
MULLIKEN ATOMIC CHARGES OF CBMA CALCULATED BY DFT/B3LYP/6-311G(d,p) FOR DIFFERENT SOLVENTS

| Atoms | Gas | Methanol | Ethanol | Benzene | DClE | DMSO |
|---|---|---|---|---|---|---|
| 1C | 0.021 | 0.015 | 0.015 | 0.018 | 0.015 | 0.015 |
| 2C | -0.065 | -0.067 | -0.068 | -0.067 | -0.068 | -0.067 |
| 3C | -0.147 | -0.156 | -0.157 | -0.151 | -0.155 | -0.157 |
| 4C | -0.018 | -0.034 | -0.033 | -0.024 | -0.032 | -0.034 |
| 5C | 0.021 | 0.015 | 0.014 | 0.018 | 0.015 | -14 |
| 6C | -0.231 | -0.238 | -0.237 | -0.234 | -0.237 | -0.238 |
| 7H | 0.119 | 0.136 | 0.135 | 0.126 | 0.134 | 0.136 |
| 8H | 0.095 | 0.119 | 0.119 | 0.105 | 0.117 | 0.12 |
| 9H | 0.109 | 0.109 | 0.109 | 0.11 | 0.109 | 0.109 |
| 10H | 0.122 | 0.136 | 0.136 | 0.129 | 0.135 | 0.137 |
| 11Cl | -0.066 | -0.079 | -0.079 | -0.073 | -0.078 | -0.079 |
| 12C | 0.139 | 0.143 | 0.142 | 0.14 | 0.142 | 0.143 |
| 13H | 0.073 | 0.098 | 0.097 | 0.082 | 0.094 | 0.098 |
| 14N | -0.324 | -0.343 | -0.342 | -0.331 | -0.341 | -0.343 |
| 15C | 0.049 | 0.04 | 0.041 | 0.045 | 0.041 | 0.04 |
| 16C | -0.052 | -0.073 | -0.073 | -0.061 | -0.071 | -0.074 |
| 17C | -0.068 | -0.081 | -0.081 | -0.074 | -0.079 | -0.081 |
| 18C | -0.092 | -0.111 | -0.111 | -0.1 | -0.011 | -0.011 |
| 19H | 0.098 | 0.105 | 0.105 | 0.101 | 0.104 | 0.105 |
| 20C | -0.0139 | -0.151 | -0.15 | -0.145 | -0.149 | -0.15 |
| 21H | 0.099 | 0.121 | 0.12 | 0.107 | 0.118 | 0.121 |
| 22C | 0.175 | 0.172 | 0.173 | 0.174 | 0.173 | 0.172 |
| 23H | 0.104 | 0.113 | 0.112 | 0.108 | 0.112 | 0.113 |
| 24H | 0.104 | 0.129 | 0.128 | 0.114 | 0.126 | 0.129 |
| 25C | -0.132 | -0.14 | -0.14 | -0.136 | -0.139 | -0.14 |
| 26H | 0.13 | 0.137 | 0.137 | 0.134 | 0.136 | 0.137 |
| 27H | 0.11 | 0.123 | 0.122 | 0.116 | 0.121 | 0.123 |
| 28H | 0.111 | 0.123 | 0.123 | 0.116 | 0.121 | 0.123 |
| 29O | -0.346 | -0.36 | -0.36 | -0.352 | -0.358 | -0.36 |

TABLE-9
THERMODYNAMIC PROPERTIES OF CBMA AT DIFFERENT TEMPERATURES USING B3LYP/6-11G(d, p)

| T (K) | C (cal/mol K) | S (cal/mol K) | ΔH (kcal/mol) |
|---|---|---|---|
| 100 | 24.993 | 83.338 | 1.667 |
| 200 | 41.456 | 105.65 | 4.979 |
| 298.15 | 58.67 | 125.39 | 9.89 |
| 300 | 58.99 | 125.75 | 9.998 |
| 400 | 75.73 | 145.07 | 16.75 |
| 500 | 89.97 | 163.55 | 25.06 |
| 600 | 101.53 | 181.01 | 34.65 |
| 700 | 110.86 | 197.39 | 45.29 |
| 800 | 118.48 | 212.71 | 56.77 |
| 900 | 124.8 | 227.04 | 68.95 |
| 1000 | 130.09 | 240.47 | 81.69 |

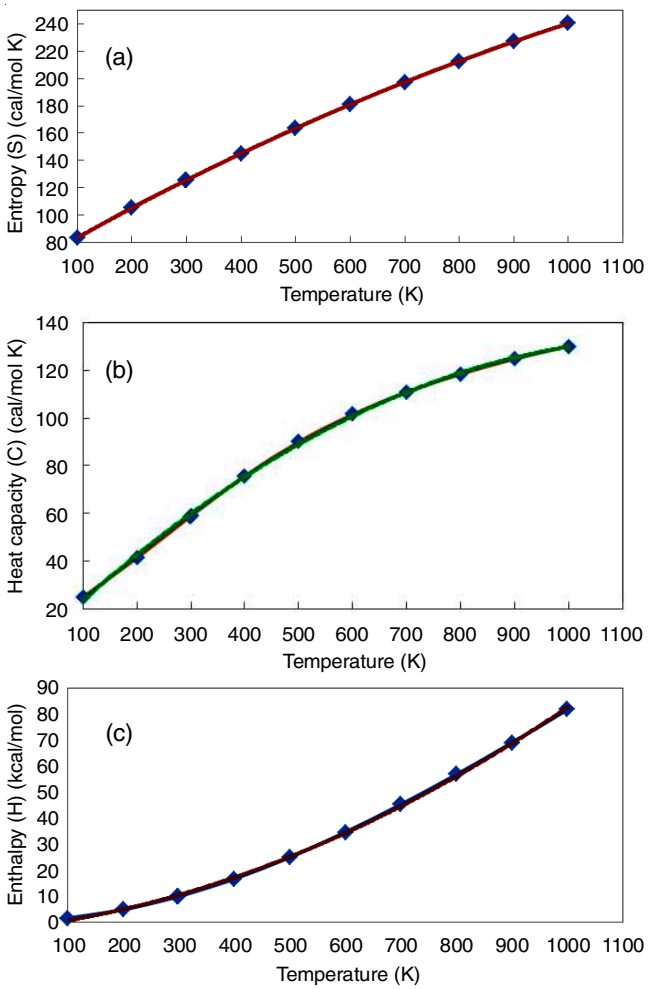


Fig. 10. Correlation graphs of (a) entropy *vs.* temperature, (b) heat capacity *vs.* temperature and (c) enthalpy *vs.* temperature for CBMA

$$S = 61.11 + 0.230T - 5 \times 10^{-5} T^2 \quad (R^2 = 1.0000) \qquad (15)$$

These data provided helpful information for the further study on CBMA molecule. All thermodynamic calculations have been done in gas phase and they could not be used in solutions.

## Conclusion

Single crystals of N-(4-chlorobenzylidene)-4-methoxy-aniline (CBMA) were grown by solution growth technique. The molecular geometry and wave numbers were calculated using HF and DFT/B3LYP with 6-311G(d,p) basis set. The FT-IR and FT-Raman spectra of CBMA were studied. The UV spectra of CBMA were studied in different solvents such as methanol, ethanol, benzene, dichloroethane and dimethyl sulfoxide. The value of the energy separation between the HOMO and LUMO was found to be very small and this energy gap gave significant information about the title compound. So, it is concluded that CBMA molecule was found to be soft. From the NBO analysis, the $\pi^* \rightarrow \pi^*$ interaction revealed the strongest stabilization to the system. The calculated first order hyperpolarizability was found to be much greater than urea, which proved that the CBMA is a good non-linear optical material. The MEP map showed the maximum positive region localized around the hydrogen atoms and the maximum negative region localized on nitrogen atom. The chemical hardness, chemical softness and electrophilicity index were calculated. The thermodynamic properties like heat capacity, enthalpy and entropy were calculated in the temperature range from 100 to 1000 K.

## ACKNOWLEDGEMENTS

One of the authors (A.S.H) is grateful to Science and Engineering Research Board (SERB), Department of Science and Technology (DST), Government of India for sanctioning the financial assistance for the project with F.No. SR/FTP/PS-049/2013.

## REFERENCES

1. F.F. Jian, R.R. Zhuang, K.F. Wang, P.S. Zhao and H. Xiao, *Acta Cryst.*, E62, o3198 (2006); https://doi.org/10.1107/S1600536806025074.
2. M.T.H. Tarafder, M.A. Ali, D.J. Wee, K. Azahari, S. Silong and K. Crouse, *Transition Met. Chem.*, **25**, 456 (2000); https://doi.org/10.1023/A:1007062409973.
3. P. Deschamps, P.P. Kulkarni and B. Sarkar, *Inorg. Chem.*, **42**, 7366 (2003); https://doi.org/10.1021/ic034760x.
4. Z. Rozwadowski, E. Majewski, T. Dziembowska and P.E. Hansen, *J. Chem. Soc. Perkin Trans. II*, 2809 (1999); https://doi.org/10.1039/a903200b.
5. S. Kumar, D.G. Ladha, P.C. Jha and N.K. Shah, *Int. J. Corros.*, **Article ID 819643** (2013); https://doi.org/10.1155/2013/819643.
6. D.S. Chemla and J. Zyss, Nonlinear Optical Properties of Organic Molecules and Crystals, Academic Press, New York, 1987.
7. P.N. Prasad and D.J. Williams, Introduction to Nonlinear Optical Effects in Organic Molecules and Polymers, Wiley, New York (1991).
8. P. Srinivasan, T. Kanagasekaran and R. Gopalakrishnan, *Cryst. Growth Des.*, **8**, 2340 (2008); https://doi.org/10.1021/cg701143n.
9. G. Zhang, M. Liu, D. Xu, D. Yuan, W. Sheng and J. Yao, *J. Mater. Sci. Lett.*, **19**, 1255 (2000); https://doi.org/10.1023/A:1006733831655.
10. R.W. Munn and C.N. Ironside, Principles and Applications of Non-Linear Optical Materials, Chapman and Hall, London (1993).
11. K. Naseema, V. Rao, K.V. Sujith and B. Kalluraya, *Curr. Appl. Phys.*, **10**, 1236 (2010); https://doi.org/10.1016/j.cap.2010.02.050.
12. S. Leela, K. Ramamurthi and G. Bhagavannarayana, *Spectrochim. Acta A*, **74**, 78 (2009); https://doi.org/10.1016/j.saa.2009.05.028.
13. S. Leela, T.D. Rani, A. Subashini, S. Brindha, R.R. Babu and K. Ramamurthi, *Arab. J.Chem.*, **10(Suppl.2)**, S3974 (2017); https://doi.org/10.1016/j.arabjc.2014.06.008.
14. K. Srinivasan, K. Sankaranarayanan, S. Thangavelu and P. Ramasamy, *J. Cryst. Growth*, **212**, 246 (2000); https://doi.org/10.1016/S0022-0248(00)00300-6.

15. A. Subashini, G. Bhagavannarayana and K. Ramamurthi, *Spectrochim. Acta A*, **82**, 91 (2011); https://doi.org/10.1016/j.saa.2011.07.004.
16. X.Y. Ren, Y.F. Ding and F.F. Jiana, *Acta Cryst.,* **E64**, o1793 (2008); https://doi.org/10.1107/S1600536808026111.
17. P. Hohenberg and W. Kohn, *Phys. Rev.*, **136(3B)**, B864 (1964); https://doi.org/10.1103/PhysRev.136.B864.
18. A. Becke, *J. Chem. Phys.*, **98**, 5648 (1993); https://doi.org/10.1063/1.464913.
19. C. Lee, W. Yang and R.G. Parr, *Phys. Rev.*, **B37**, 785 (1988); https://doi.org/10.1103/PhysRevB.37.785.
20. M.J. Frisch, G.W. Trucks, H.B. Schlegel, G.E. Scuseria, M.A. Robb, J.R. Cheeseman, G. Scalmani, V. Barone, B. Mennucci, G.A. Petersson, H. Nakatsuji, M. Caricato, X. Li, H.P. Hratchian, A.F. Izmaylov, J. Bloino, G. Zheng, J.L. Sonnenberg, M. Hada, M. Ehara, K. Toyota, R. Fukuda, J. Hasegawa, M. Ishida, T. Nakajima, Y. Honda, O. Kitao, H. Nakai, T. Vreven, J.A. Montgomery Jr., J.E. Peralta, F. Ogliaro, M. Bearpark, J.J. Heyd, E. Brothers, K.N. Kudin, V.N. Staroverov, R. Kobayashi, J. Normand, K. Raghavachari, A. Rendell, J.C. Burant, S.S. Iyengar, J. Tomasi, M. Cossi, N. Rega, N.J. Millam, M. Klene, J.E. Knox, J.B. Cross, V. Bakken, C. Adamo, J. Jaramillo, R. Gomperts, R.E. Stratmann, O. Yazyev, A.J. Austin, R. Cammi, C. Pomelli, J.W. Ochterski, R.L. Martin, K. Morokuma, V.G. Zakrzewski, G.A. Voth, P. Salvador, J.J. Dannenberg, S. Dapprich, A.D. Daniels, Ö. Farkas, J.B. Foresman, J.V. Ortiz, J. Cioslowski and D.J. Fox, Gaussian 09, Revision A.1, Gaussian Inc., Wallingford CT (2009).
21. E.D. Glendening, C.R. Landis and F. Weinhold, *Comput. Mol. Sci.*, **2**, 1 (2012); https://doi.org/10.1002/wcms.51.
22. D.A. Kleinman, *Phys. Rev.*, **126**, 1977 (1962); https://doi.org/10.1103/PhysRev.126.1977.
23. S. Shen, G.A. Guirgis and J.R. Durig, *Struct. Chem.*, **12**, 33 (2001); https://doi.org/10.1023/A:1009258017813.
24. D. Michalska and R. Wysokinski, *Chem. Phys. Lett.*, **403**, 211 (2005); https://doi.org/10.1016/j.cplett.2004.12.096.
25. L.E. Sutton, Tables of Interatomic Distances, Chemical Society, London (1958).
26. S. Muthu, G. Ramachandran and J. Uma maheswari, *Spectrochim. Acta A*, **93**, 214 (2012); https://doi.org/10.1016/j.saa.2012.02.107.
27. G. Varsanyi, Vibrational Spectra of Benzene Derivatives, Academic Press, NewYork (1969).
28. B.C. Smith, Infrared Spectral Interpretation, A Systematic Approach, CRC Press, Washington DC (1999).
29. N.P.G. Roeges, A Guide to the Complete Interpretation of Infrared Spectra of Organic Structures, Wiley, New York (1994).
30. A.S. El-Shahawy, S.M. Ahmed and N.K. Sayed, *Spectrochim. Acta A*, **66**, 143 (2007); https://doi.org/10.1016/j.saa.2006.02.034.
31. R.M. Silverstein, G.C. Bassler and T.C. Morril, Spectrometric Identification of Organic Compounds, John Wiley & Sons Inc., Singapore, edn 5 (1991).
32. E.F. Mooney, *Spectrochim. Acta A*, **19**, 877 (1963); https://doi.org/10.1016/0371-1951(63)80175-7.
33. N.B. Colthup, L.H. Daly and S.E. Wiberley, Introduction to Infrared and Raman Spectroscopy, Academic Press, Boston, edn 3 (1990).
34. P. Pazdera, H. Divisová, H. Havlisová and P. Borek, *Molecules*, **5**, 189 (2000); https://doi.org/10.3390/50200189.
35. H. Divisová, H. Havlisová, P. Borek and P. Pazdera, *Molecules*, **5**, 1166 (2000); https://doi.org/10.3390/51001166.
36. M. Snehalatha, C. Ravikumar, I.H. Joe, N. Sekar and V.S. Jayakumar, *Spectrochim. Acta A*, **72**, 654 (2009); https://doi.org/10.1016/j.saa.2008.11.017.
37. K. Govindarasu, E. Kavitha and N. Sundaraganesan, *Spectrochim. Acta A*, **133**, 417 (2014); https://doi.org/10.1016/j.saa.2014.06.040.
38. C. Andraud, T. Brotin, C. Garcia, F. Pelle, P. Goldner, B. Bigot and A. Collet, *J. Am. Chem. Soc.*, **116**, 2094 (1994); https://doi.org/10.1021/ja00084a055.
39. V.M. Geskin, C. Lambert and J. Bredas, *J. Am. Chem. Soc.*, **125**, 15651 (2003); https://doi.org/10.1021/ja035862p.
40. M. Karabacak, Z. Cinar and M. Cinar, *Spectrochim. Acta A*, **85**, 241 (2012); https://doi.org/10.1016/j.saa.2011.10.001.
41. K. Govindarasu and E. Kavitha, *Spectrochim. Acta A*, **122**, 130 (2014); https://doi.org/10.1016/j.saa.2013.10.122.
42. T. Vijayakumar, I.H. Joe, C.P. Reghunadhan Nair and V.S. Jayakumar, *Chem. Phys.*, **343**, 83 (2008); https://doi.org/10.1016/j.chemphys.2007.10.033.
43. M.A. Palafox, *Int. J. Quantum Chem.*, **77**, 661 (2000); https://doi.org/10.1002/(SICI)1097-461X(2000)77:3<661::AID-QUA7>3.0.CO;2-J.
44. I. Fleming, Frontier Orbitals and Organic Chemical Reactions, John Wiley & Sons, New York (1976).
45. T. Karakurt, M. Dincer, A. Cetin and M. Sekerci, *Spectrochim. Acta A*, **77**, 189 (2010); https://doi.org/10.1016/j.saa.2010.05.006.
46. C.H. Choi and M. Kertesz, *J. Phys. Chem. A*, **101**, 3823 (1997); https://doi.org/10.1021/jp970620v.
47. D.F.V. Lewis, C. Ioannides and D. Parke, *Xenobiotica*, **24**, 401 (1994); https://doi.org/10.3109/00498259409043243.
48. V. Balachandran and V. Karunakaran, *Spectrochim. Acta A*, **106**, 284 (2013); https://doi.org/10.1016/j.saa.2012.12.070.
49. P. Politzer and J.S. Murray, *Theor. Chem. Acc.*, **108**, 134 (2002); https://doi.org/10.1007/s00214-002-0363-9.
50. R. Parr, L. Szentpaly and S. Liu, *Am. Chem. Soc.*, **121**, 1922 (1999); https://doi.org/10.1021/ja983494x.
51. P.K. Chattaraj, B. Maiti and U. Sarkar, *J. Phys. Chem. A*, **107**, 4973 (2003); https://doi.org/10.1021/jp034707u.
52. K. Govindarasu and E. Kavitha, *J. Mol. Struct.*, **1088**, 70 (2015); https://doi.org/10.1016/j.molstruc.2015.02.008.
53. T.A. Koopmans, *Physica*, **1**, 104 (1934); https://doi.org/10.1016/S0031-8914(34)90011-2.
54. D.A. Dhas, I.H. Joe, S.D.D. Roy and T.H. Freeda, *Spectrochim. Acta A*, **77**, 36 (2010); https://doi.org/10.1016/j.saa.2010.04.020.
55. J.B. Ott and J. Boerio-Goates, Chemical Thermodynamics: Advanced Applications, Calculations from Statistical Thermodynamics, Academic Press (2000).